STATIC CAPACITY PREDICTION BY DYNAMIC METHODS FOR THREE BORED PILES

By Jean-Louis Briaud,[1] Fellow, ASCE, Marc Ballouz,[2] and George Nasr,[3] Members, ASCE

ABSTRACT: Three bored piles were built and tested at the National Geotechnical Experimentation Sites, at Texas A&M University, to gather data on the reliability of large-strain dynamic methods to predict the static capacity of bored piles. The three piles had a nominal diameter of 0.915 m, a nominal length of 10 m, and some planned and unplanned defects. The piles were first subjected to a static load test and then four companies were asked to perform dynamic tests—namely, Statnamic and drop weight tests—and predict the static load test results. The paper shows the comparison between predicted and measured results.

INTRODUCTION

Bored piles are a very popular and cost-effective type of foundation. The major objective of this project was to evaluate the ability of large-strain dynamic testing methods—namely, the drop weight method and the Statnamic method—to predict the static capacity of bored piles. This objective was achieved by constructing two bored piles in sand and one bored pile in clay at the National Geotechnical Experimentation Sites at Texas A&M University, inviting various companies to perform large-strain dynamic testing (drop weight and Statnamic) and make "class A" predictions of the static capacity of the three bored piles; this static capacity was measured by conventional static load tests. Similar tests were performed in California prior to the Texas A&M University tests, but, for the California tests, the predicting companies knew the load test results before making their predictions. These predictions are, therefore, not "class A" predictions and are not reported here. They can be found in Baker et al. (1993). That reference also includes the Texas A&M University tests.

SITE AND SOIL DESCRIPTION

The sites were the two National Geotechnical Experimentation Sites at Texas A&M University: Sand and Clay. The top layers, 12.5 m at the sand site and 6.5 m at the clay site, are 100,000-year-old river deposits, while the hard clay underlying both sites is a 45,000,000-year-old marine shale that was deposited by a series of transgressions and regressions of the Gulf of Mexico. The sand is a medium-dense silty sand with the properties shown in Fig. 1(a). The clay is a very stiff plastic clay with the properties shown in Fig. 1(b). Details of the soil properties are in Briaud (1997) and Simon and Briaud (1996).

BORED PILES CONSTRUCTION

A total of nine bored piles were constructed, piles 1–5 at the sand site and piles 6–9 at the clay site. All piles were planned to be 0.915 m in diameter and varied in length between 10.7 and 24.1 m. At the clay site the piles were drilled dry while at the sand site they were drilled dry to start and then completed under slurry. Details of the construction are in Ballouz et al. (1991) and the construction schedule is given in Table 1. This table also gives the testing sequence for each pile. The piles were constructed by following good drilling and construction practices including desanding of the drilling mud and minimizing slurry stagnation between the end of drilling and the beginning of concreting. Pile 2 at the sand site was an exception.

Pile 2 (Fig. 2) at the sand site was purposely built with a mud cake on the side wall, a soft bottom, and a concrete contamination at 5.3 m below the top of the pile. The mud cake was approximately 15 mm thick and was created by leaving the bentonite drilling mud in the open hole for 60 h; the mud cake was extremely slick. The soft bottom was created when the sand mixed with the drilling slurry settled at the bottom of the hole during the 60 h and formed an approximately 0.3-

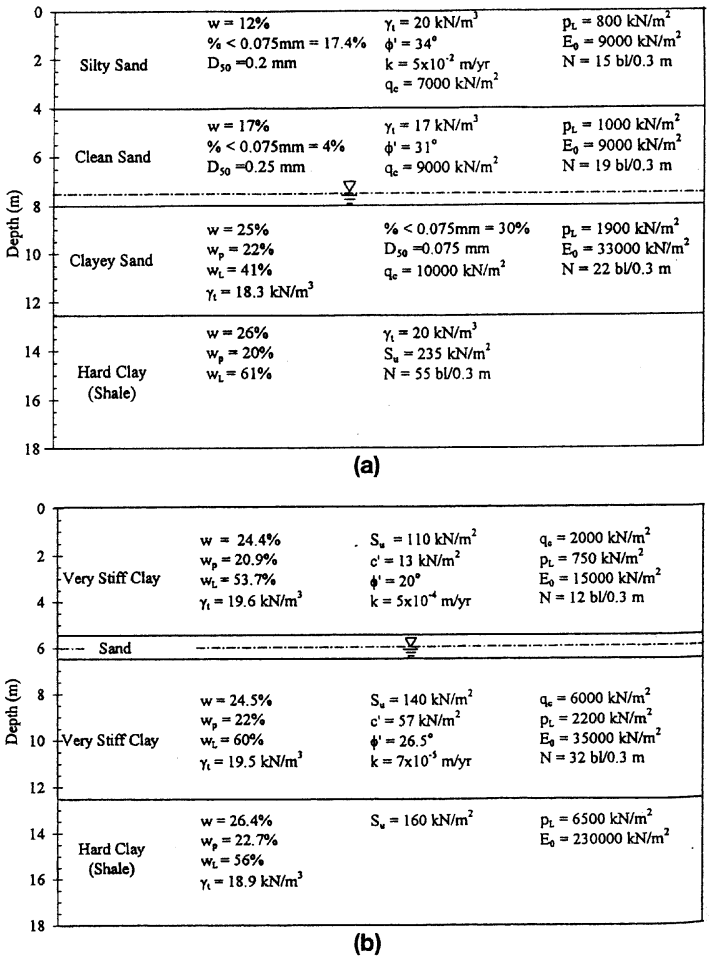

FIG. 1. Summary of Soil Properties at NGES-TAMU Sites: (a) Sand Site; (b) Clay Site

[1]Spencer J. Buchanan Prof., Dept. of Civ. Engrg., Texas A&M Univ., College Station, TX 77843-3136.

[2]Dir., Institute for Geotechnics & Materials, P.O. Box 166-864, Achrafieh, Beirut, Lebanon.

[3]Engr., 633 Bay #202, Toronto, Ontario, M5G2G4, Canada.

Note. Discussion open until December 1, 2000. To extend the closing date one month, a written request must be filed with the ASCE Manager of Journals. The manuscript for this paper was submitted for review and possible publication on January 26, 1998. This paper is part of the ***Journal of Geotechnical and Geoenvironmental Engineering***, Vol. 126, No. 7, July, 2000. ©ASCE, ISSN 1090-0241/00/0007-0640–0649/$8.00 + $.50 per page. Paper No. 17460.

TABLE 1. Construction and Testing Schedule

Pile number (1)	Site (2)	Drilling (3)	Concreting (4)	Static test 1 (5)	Statnamic test (6)	Drop weight test (7)	Static test 2 (8)
2	sand	Nov. 16, 1990	Nov. 19, 1990	Nov. 28, 1990	Dec. 4, 1990	Dec. 6, 1990	Dec. 8, 1990
4	sand	Nov. 19, 1990	Nov. 19, 1990	Nov. 30, 1990	Dec. 5, 1990	Dec. 7, 1990	—
7	clay	Nov. 15, 1990	Nov. 15, 1990	Dec. 3, 1990	Dec. 7, 1990	Dec. 8, 1990	—

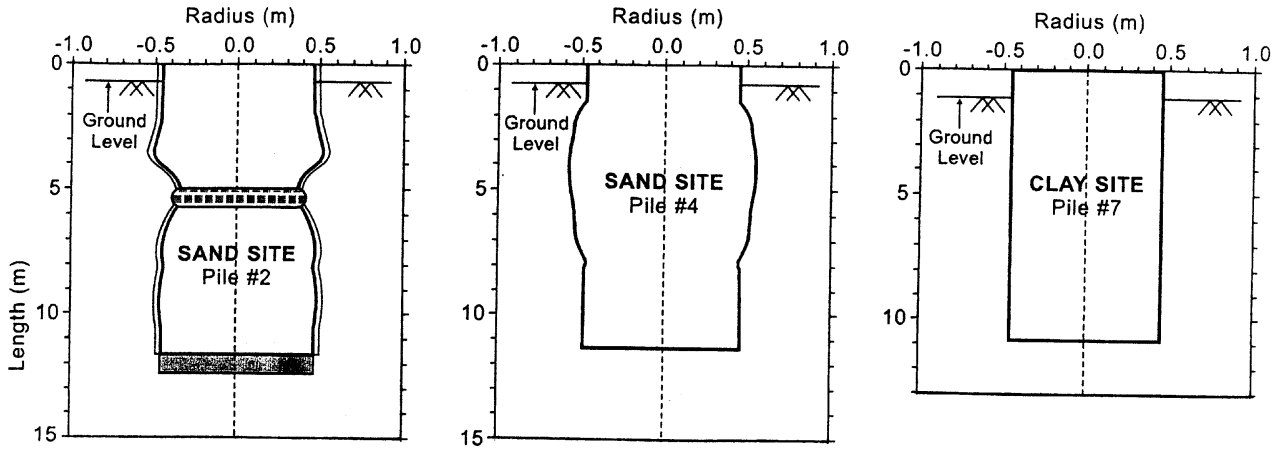

FIG. 2. Bored Piles at NGES-TAMU Sites

m-thick layer of loose clayey sand. The concrete contamination at 5.3 m occurred when the concrete tremie was purposely pulled above the concrete-mud interface during the concreting process. An unplanned defect occurred at 5.0 m below the top of the pile and resulted in a 45% necking or reduction in area.

Pile 4 (Fig. 2) at the sand site was planned as a no-defect pile with no drilling mud stagnation and proper drilling mud desanding to avoid a soft bottom; however, caving of the side walls created an unplanned bulging defect resulting in a 10% average increase in diameter between 1.2 and 7.5 m below the top of the pile.

Pile 7 (Fig. 2) at the clay site was planned and executed as a perfect pile. The shapes of piles 2, 4, and 7 as obtained from the concrete volume curves are shown in Fig. 2. Piles 2, 4, and 7 were subjected to static load testing, Statnamic testing, and drop weight testing. The testing sequence is given by the dates in Table 1.

PILE INSTRUMENTATION

In order to obtain the load distribution in the pile during the static load test, sister bars were installed. A sister bar [Fig. 3(a)] consisted of a 1.4-m-long number 4 reinforcement bar with a vibrating wire strain gauge welded to the steel in the center of the bar. The sister bars were tied to the tie bars of the reinforcement cage away from the longitudinal bars to achieve a better bonding with the concrete. In pile 2 and pile 4, the strain gauges of the sister bars were located at 3.2, 6.3, and 9.3 m below the pile top. In pile 7, they were at 4.7 and 9.2 m below the pile top. The strain gauge of each sister bar gives the strain ε in the concrete and in the steel and therefore the load P in the pile at that depth:

$$P = A_c E_c \varepsilon + A_S E_S \varepsilon \quad (1)$$

where A_c and A_S = concrete and steel cross section areas, respectively, and E_c and E_S are the concrete and steel modulus of elasticity, respectively.

Removable extensometers were also used to measure the load in the piles. Two diametrically opposed 76 mm ID PVC closed-end pipes were tied to the reinforcement cage of piles

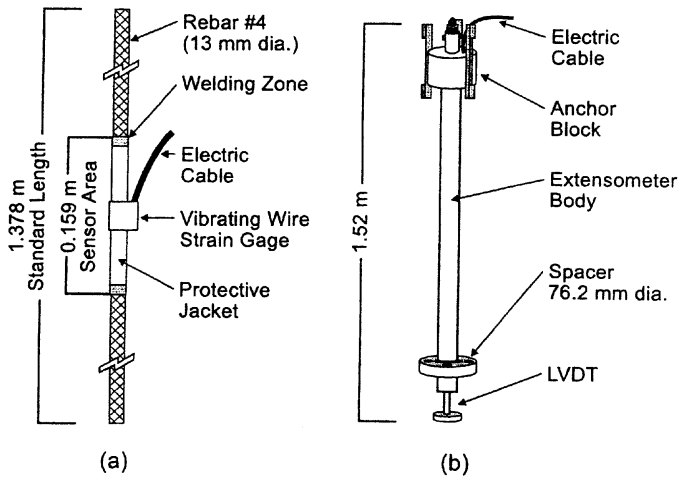

FIG. 3. Pile Instrumentation: (a) Sister Bars; (b) Removable Extensometers

2, 4, and 7. The removable extensometers [Fig. 3(b)] were 1.525 m long with an expanding anchor at one end and a displacement transducer at the other. Five extensometers were placed on top of each other in each of the two PVC pipes before the load tests. The anchors were expanded mechanically to connect the extensometers to the pile; each displacement transducer was resting on the anchor of the extensometer below it. The displacement transducer gives the change in length of the 1.525 m segment of pile and therefore the strain from which the load in the pile is calculated. The advantage of the extensometers is that they can be reused; the limitation is that the change in length of the 1.525 m segment of pile must be larger than the smallest detectable movement for the displacement transducer.

STATIC LOAD TESTS AND LOAD-SETTLEMENT CURVES

The load test setup is illustrated in Fig. 4. The load was measured by using a 10,000 kN load cell, and the displacement

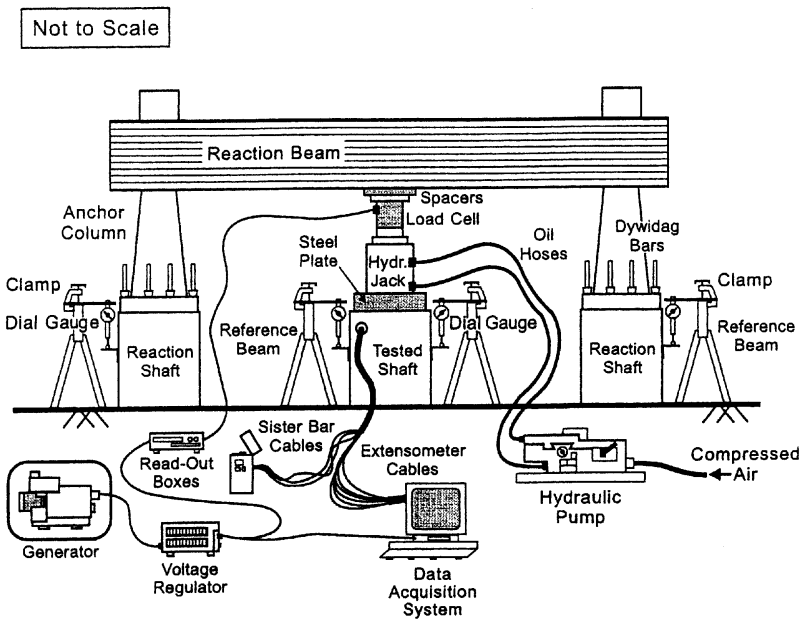

FIG. 4. Schematic View of Static Load Test

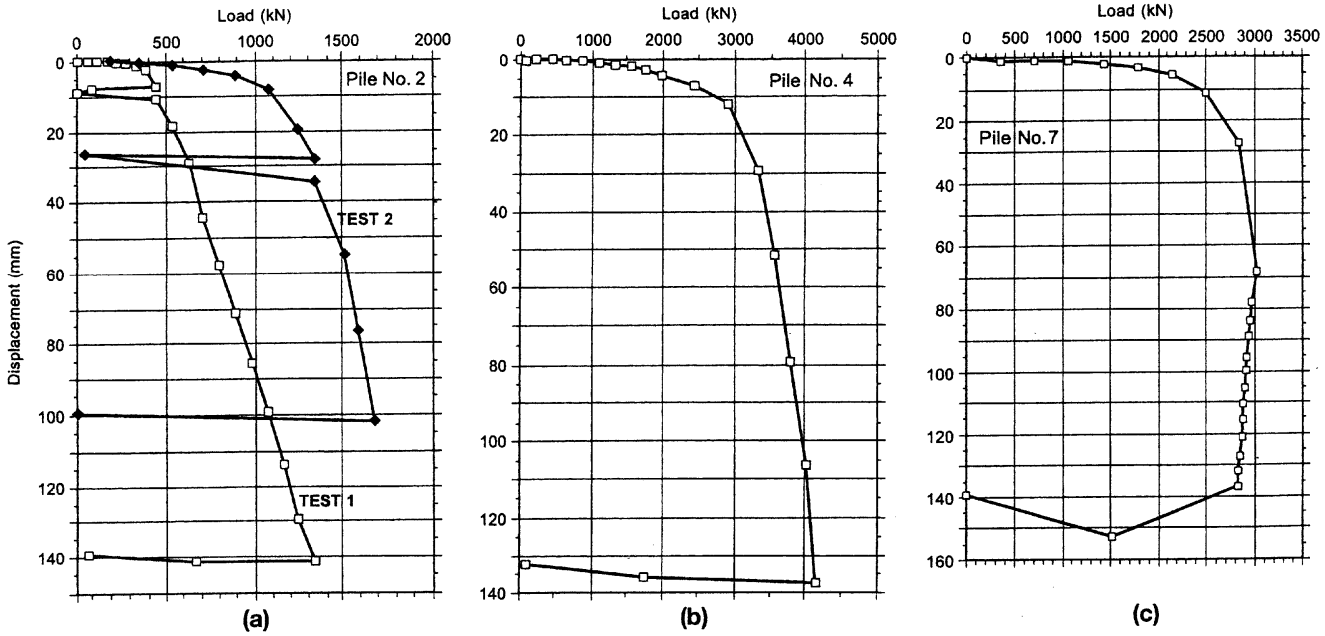

FIG. 5. Load-Settlement Curves for Static Load Tests: (a) Pile 2; (b) Pile 4; (c) Pile 7

was measured with dial gauges attached to reference beams with supports placed at least 5 pile diameters away. The strain in the sister bars and the displacement of the extensometers were also recorded during the tests.

The load was applied in a series of 15 min load steps. During each load step, the displacement and the load at the pile top, as well as the strain in the sister bars and the displacement of the extensometers, were recorded at 1, 3, 7, and 15 min. The load steps were chosen as one tenth of the estimated pile capacity and the piles were pushed to about 140 mm of penetration.

Piles 2, 4, and 7 were load tested before any dynamic tests took place. Pile 2 was subjected to a second static load test after the dynamic tests to confirm the capacity. The results of the tests are shown in Fig. 5 for the 15 min readings. There are many ways to define pile capacity from a load settlement curve (e.g., Fellenius 1975). Capacities defined according to the Davisson criterion ($D/120 + 3.8$ mm $+ PL/AE$) and the $D/10$ criterion ($D/10 + PL/AE$) are shown in Table 2. The diameter of the pile is D, the length of the pile is L, the cross section area of the pile is A, the modulus of the pile material is E, and the load applied is P. On the average, the Davisson capacity is equal to 0.72 times the $D/10$ capacity and corresponds to an average pile top penetration of 12 mm; such a small displacement is in most instances an acceptable settlement and much too small for a capacity determination. The $D/10$ criterion, on the other hand, corresponds to an average pile top penetration of 93 mm and, in the writer's opinion, should be favored for capacity determination.

LOAD DISTRIBUTION IN PILES

The load distribution in the piles was obtained separately from the sister bars and from the extensometers. The load distributions according to the sister bars for the four load tests

TABLE 2. Observations on Static Capacity of Piles

Parameters (1)	Sand Site			Clay Site
	Pile 2 (test 1) (2)	Pile 2 (test 2) (3)	Pile 4 (4)	Pile 7 (5)
Capacity ($D/10$ + PL/AE)	1,068	1,602	4,004	3,025
Capacity (Davisson)	472	1,112	2,892	2,491
Point load (kN)($D/10$ + PL/AE)	590	770	700	1,050
Friction load (kN) ($D/10$ + PL/AE)	178	832	3,304	1,975
Point pressure, q_{max} (kPa)	1,355	1,172	1,065	1,598
Friction stress, f_{max} (kPa)	5.7	26.6	108.6	71.7
q_c for point (kPa)	10,000	10,000	10,000	6,000
q_c for friction (kPa)	8,400	8,400	8,400	4,000
P_L for point (kPa)	1,900	1,900	1,900	2,200
P_L for friction (kPa)	1,100	1,100	1,100	1,475
N for point (bpf)	22	22	22	32
N for friction (bpf)	18	18	18	22
S_u for point (kPa)	—	—	—	140
S_u for friction (kPa)	—	—	—	125
σ'_{ov} for point (kPa)	159	159	156	162
σ'_{ov} for friction (kPa)	90.6	90.6	90.2	92.4
q_{max}/q_c	0.135	0.117	0.106	0.266
f_{max}/q_c	0.000679	0.00317	0.0129	0.0179
q_{max}/P_L	0.713	0.617	0.561	0.726
f_{max}/P_L	0.00518	0.0242	0.0987	0.0486
q_{max}/N	61.6	53.3	48.4	49.9
f_{max}/N	0.32	1.48	6.0	3.26
q_{max}/S_u	—	—	—	11.4
f_{max}/S_u	—	—	—	0.574
q_{max}/σ'_{ov}	8.52	7.37	6.83	9.86
f_{max}/σ'_{ov}	0.063	0.29	1.20	0.78

on the three piles are shown in Figs. 6 and 7. The distributions from the extensometers confirmed the general trend.

As can be seen from the load-settlement curves on Fig. 5, pile 2 carried much less load than pile 4 even though they have the same diameter and the same length in the same soil. The $D/10$ capacity of pile 2 is about four times smaller than the $D/10$ capacity of pile 4. The soft bottom defect on pile 2 does not seem to be a true defect, since the point loads are (Figs. 6 and 7) 880 kN for pile 2 and 700 kN for pile 4 at the $D/10$ criterion according to the sister bars. It is likely that the weight of the wet concrete recompressed the soft bottom to stiffen it back to the original condition or else the wet concrete permeated or mixed with the soft bottom and turned it into an integral part of the pile.

The friction load is much lower for pile 2 than it is for pile 4: 190 kN for pile 2 and 3,300 kN for pile 4 at the $D/10$ criterion, according to the sister bars. This very large difference is due to the mud cake and to the bulging configuration of the shaft of pile 4. The bulging of pile 4 increased the diameter from 0.915 to 1.10 m at the largest point of the bulb; this corresponds to an increase in cross-section area from 0.66 m^2 to 0.95 m^2. The increase in friction capacity due to the bulging of pile 4 can be estimated as the sum of the bearing capacity of the sand (obtained from the point measurements at the $D/10$ criterion) times the difference in area (700 kN/0.66 m^2 (0.95 − 0.66) = 307 kN) plus the increase in friction due to the increase in shaft area from a depth of 1.2 m to 7.5 m ($1.10 - 0.915/2 \times \pi(7.5 - 1.2) \times 108.6 = 199$ kN). This increase in friction (307 + 199 = 506 kN) is far from explaining much of the difference in friction between pile 2 and pile 4. Therefore, most of the loss in friction is attributed to the thick mud cake on pile 2, which decreases the friction load by a factor of about 15. This underscores the great importance of avoiding slurry stagnation.

Another observation is that the load settlement curves of the 2 bored piles in sand did not plunge while the one in clay did. Table 2 shows a number of results related to the static capacity of the piles defined at $D/10$ + PL/AE, including classical relationships to the soil parameters.

Residual stresses in bored piles after construction are usually considered to be insignificant; however, they can be induced by a load test. Residual stresses do not affect the plunging load of a pile but do affect the initial slope of the load settlement curve and the load distribution in a pile (Briaud and Tucker 1984). Static load test 2 on pile 2 started with residual stresses induced by previous testing. This is in part why the initial slope of the load settlement curve is stiffer. The load distribution shown on Fig. 6(b) does not include the residual loads; if it is assumed that the point and friction loads for test 2 are the same as for test 1, the residual point load in test 2 is 180 kN [1,000 kN (820 kN on Fig. 6)] or about 18% of the

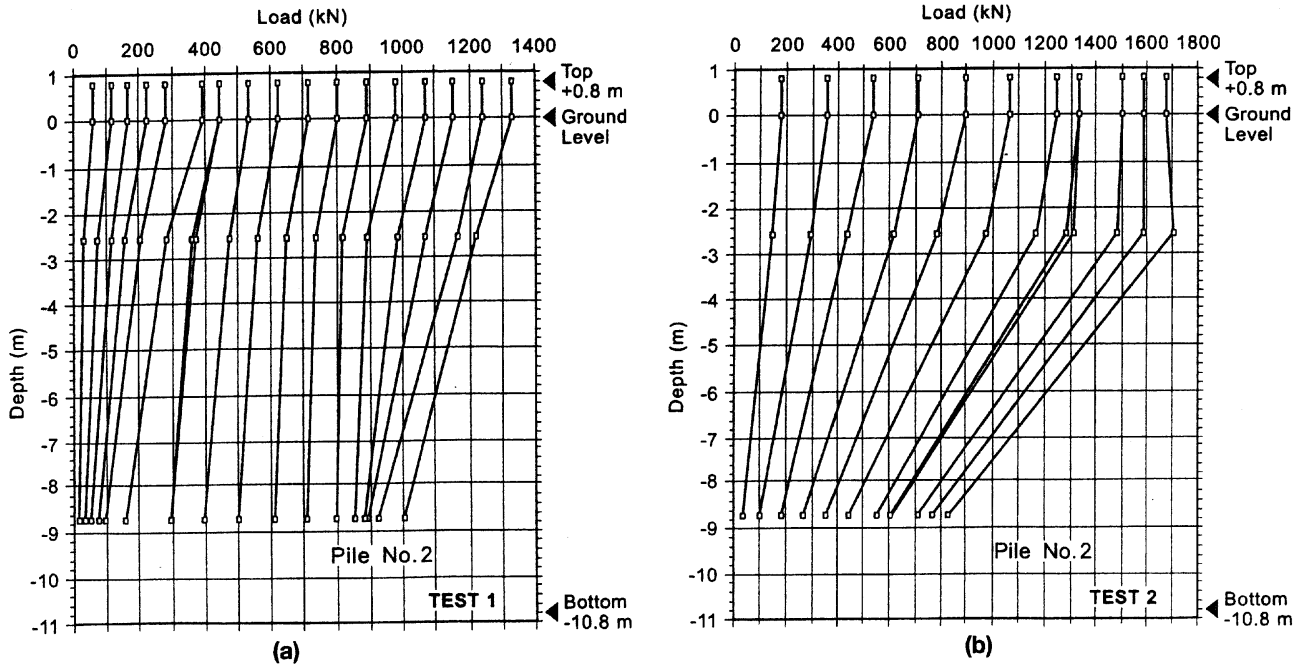

FIG. 6. Load versus Depth Profiles for Pile 2: (a) Test 1; (b) Test 2

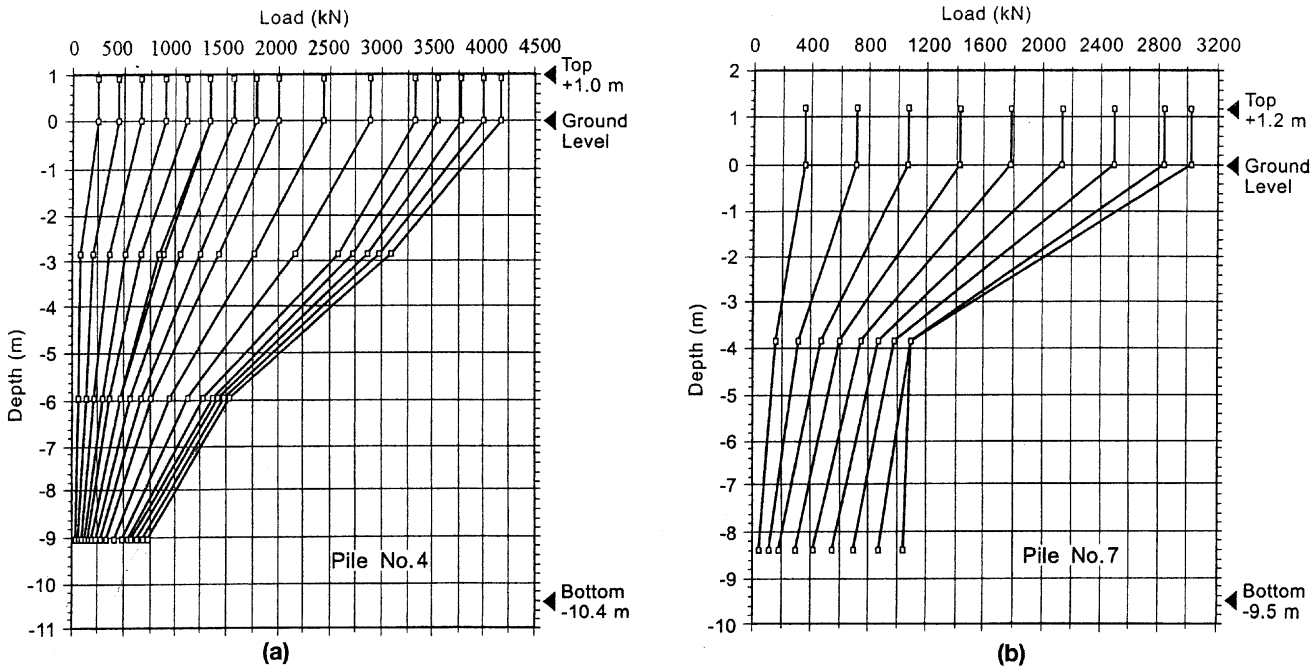

FIG. 7. Load versus Depth Profiles for (a) Pile 4; (b) Pile 7

point load. This is consistent with previous findings (Briaud and Tucker 1984a).

STATNAMIC TESTING

The Statnamic test [Bermingham and Janes 1989; Horvath et al. 1990; El Naggar and Novak (1991 (Fig. 8)] was performed by the Berminghammer Corporation (Berninghammer 1991). The test consists of placing a reaction mass on top of the bored pile to be tested. Between the pile and the reaction mass are a load cell and a fuel chamber. The solid fuel propellant is ignited and propels the reaction mass upward (from

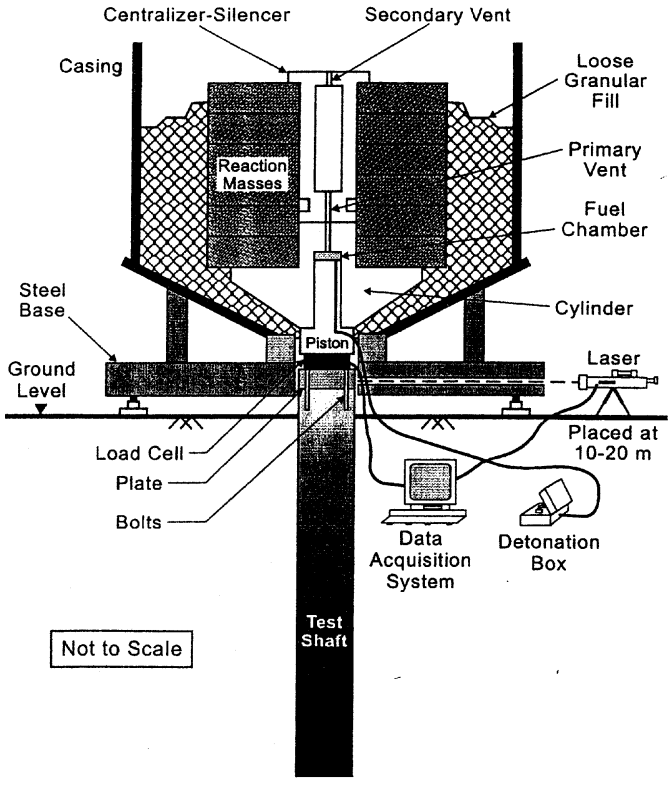

FIG. 8. Schematic View of Statnamic Test

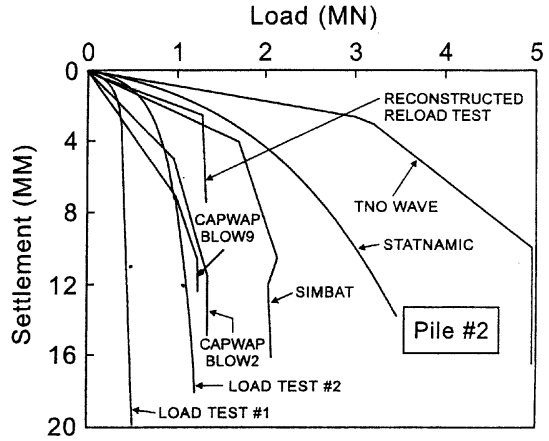

FIG. 9. Comparison between Measured and Predicted Static Load-Settlement Curves for Pile 2

1 to 3 m) while pushing the bored pile downward (from 10 to 100 mm). The loading part of the event lasts about 50 milliseconds, during which both load and displacement are recorded. The load is obtained from the load cell and the displacement is measured with a remote laser light source stationed 10 to 20 m away to minimize ground vibration; the laser beam hits a light-sensitive cell placed on the pile. The result of the test in the field is a dynamic load-settlement curve. A static load-settlement curve is then generated from the dynamic curve (Berminghammer 1991).

The Statnamic tests were performed from four to seven days after the static load tests (Table 1). The static load-settlement curves are shown in Figs. 9–11. The total penetrations varied from 13 mm for pile 7 to over 70 mm for pile 2. The maximum velocities varied from 0.32 m/s for pile 7 to 2.37 m/s for pile 2. The predictor was asked to give his best estimate of the static capacity for the piles based on his own data; these values are listed in Table 3 together with the measured static capacities according to the $D/10 + PL/AE$ criterion. The predictions for pile 4 and pile 7 are relatively close, while the predicted static capacity for the unusual pile 2 is very large. Note that a proper comparison should compare the last load applied during the preceding static test rather than the $D/10$